

The Folding Roboscooter: Structural Analysis for an Electric Scooter used in
Urban Conditions

by

Arthur J. Petron

SUBMITTED TO THE DEPARTMENT OF MECHANICAL ENGINEERING IN PARTIAL
FULLFILLMENT OF THE REQUIREMENTS FOR THE DEGREE OF

BACHELOR OF SCIENCE IN MECHANICAL ENGINEERING
AT THE
MASSACHUSETTS INSTITUTE OF TECHNOLOGY

JUNE 2008

© 2008 Arthur J. Petron. All rights reserved.

The author hereby grants to MIT permission to reproduce
and to distribute publicly paper and electronic
copies of this thesis document in whole or in part
in any medium now known or hereafter created.

Signature of Author: _____



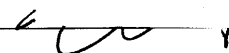
Department of Mechanical Engineering
May 9, 2008

Certified by: _____



William J Mitchell
Professor of Media Arts and Sciences
Thesis Supervisor

Certified by: _____

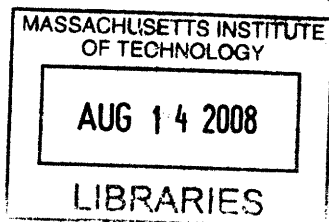


David Wallace
Professor of Mechanical Engineering
Thesis Reader

Accepted by: _____



John H. Lienhard V
Professor of Mechanical Engineering
Chairman, Undergraduate Thesis Committee



ARCHIVES

The Folding Roboscooter: Structural Analysis for an Electric Scooter used in Urban Conditions

by

Arthur J. Petron

Submitted to the Department of Mechanical Engineering
on May 9, 2008 in partial fulfillment of the
requirements for the Degree of Bachelor of Science in
Mechanical Engineering

ABSTRACT

The Roboscooter is an electric, folding scooter designed for use in dense urban areas where congestion and pollution is a problem. Already heavily used in most European cities, scooters provide cheaper, faster transportation than cars, but parking can still be difficult. By allowing the scooter to fold – reducing its footprint by more than half – and by implementing a one-way user share model that does not require scooter ownership, many of the current issues involving transportation in dense urban areas can be addressed.

As an electric vehicle, the Roboscooter's range is limited by the amount of energy it uses during travel and the current technological limitations on battery energy density. Analysis of the elements of the scooter that experience the most stress can give insights on ways to redesign key structural elements in order to make them lighter while maintaining the strength necessary for long life in a consumer environment.

The structural elements that make up the main body of the scooter are subject to cyclic fatigue due to riding conditions such as bumps, which aside from decreasing the life of structural elements, also cause the largest forces on the scooter's frame. The Roboscooter was analyzed under maximum load conditions to determine the safety factor of two of the frame components that experience the most stress: the front fork and the main folding pivot axle. Both elements were found to have a safety factor of two in their current design configurations, implying that design changes will be needed to reduce the overall weight.

Thesis Supervisor: William J. Mitchell
Title: Professor of Media Arts and Sciences

Introduction

The Roboscooter is an urban, electric, folding scooter developed by the MIT Media Laboratory in conjunction with Sanyang Motors of Taiwan (SYM) and the Industrial Technology Research Institute (ITRI). Designed with mobility and portability in mind, the scooter must be both safe and light. Not only does weight contribute to energy consumption during operation but it is also a limiting factor on the folded portability of the scooter. In order to keep weight to a minimum, the scooter's frame and other structural components must be designed to maximize weight versus strength.

The issue of weight versus strength has been a strong focus of scooter and automobile engineers since the dawn of the industry in the early 1900's. With the rise of electrical vehicle technology, weight has become an even more important factor in design because of the significantly lower power densities of battery storage technology. Analysis of the main structural and mechanical elements of the Roboscooter, including the chassis and battery pack will allow the weight versus strength characteristics of the scooter to be optimized.

There are several consumer implementation decisions that influence the design of the scooter as well. The Roboscooter, while it could possibly be used as a privately owned vehicle, is intended for use in a large-scale user share program, much like the SmartBike DC and Zipcar programs. Unlike Washington DC's bicycle program – which has no drive system – or Zipcar's program – which has a gasoline based drive system – The Roboscooter service relies on batteries to run. Unfortunately the charge time of current battery systems creates a bottleneck in the flow of scooters in and out of a parking location. In order to solve this problem, the batteries for the Roboscooter are designed to be light and easy to switch with a fully charged battery nearby.

The parking locations for the Roboscooter are to be placed strategically throughout a city. Called kiosks, these scooter rack and battery storage facilities must use as little sidewalk area as possible, as the current problem with places where scooters are already very popular like Milan, Italy and Taipei City, Taiwan suffer crowded or impassible sidewalks due to personal scooter parking. By designing the Roboscooter to fold, this problem can be reduced (see Figure 1).



Figure 1: An example of a hypothetical Roboscooter kiosk. Though not pictured here, a battery charging station would be a key part of a kiosk.

The Roboscooter Chassis

The Roboscooter currently has several design characteristics that distinguish it from typical electric scooters. The drive elements of the scooter are contained entirely in the wheel assembly, including brakes, suspension, and gearing. This configuration of the drive system is commonly referred to as a wheel-robot (see Figure 2). The advantage of the wheel-robot configuration is an increase in simplicity and modularity of the scooter's drive system. Wheel-robots do not require suspension and drive elements to be part of the main body of the scooter, which increases the flexibility and simplicity of the body design. Also, by replacing the wheel-

robot, the entire mechanical drive system is replaced, allowing for fast testing of different motor, suspension, gearing, and tire configurations.

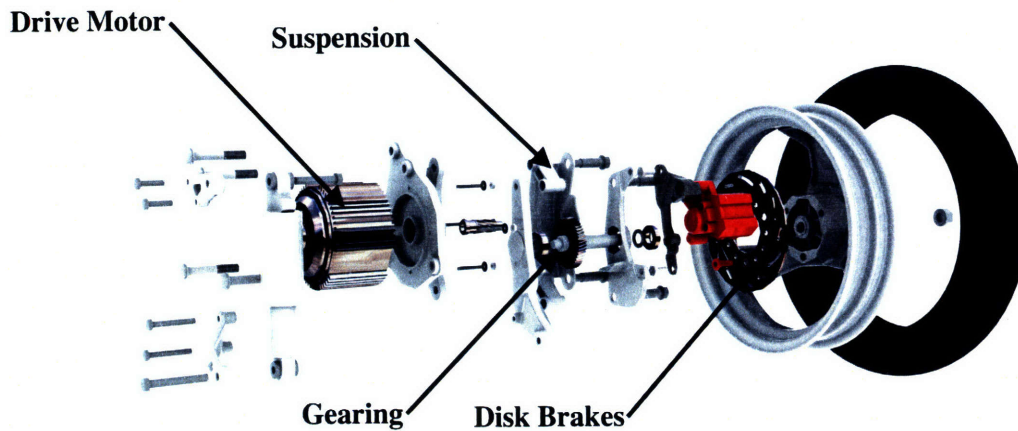


Figure 2: This exploded diagram of the current design for the Roboscooter's wheel-robot shows the components that go into the wheel hub.

The main body of the scooter contains only control electronics and batteries (see Figure 3). Because the suspension and drive materials are contained within the wheel-robot, the body of the scooter can be made of a single piece or – in the case of folding – two pieces. This configuration not only simplifies design, but also allows for weight reduction by eliminating large load-bearing joints and off the shelf components that deal with the suspension and drivetrain.

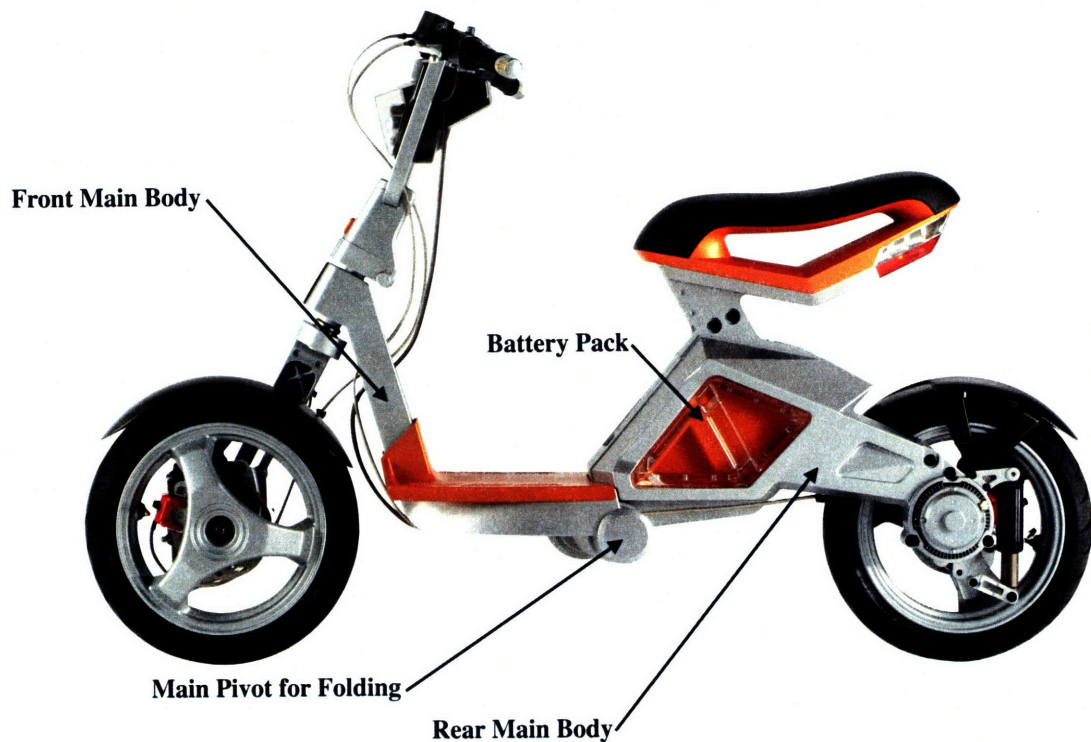


Figure 3: The main body of the Roboscooter in its current design consists of two cast aluminum pieces. Analysis of the structure of these pieces is the key to reducing the weight of the scooter.

The Roboscooter Battery Pack

As seen in Figure 3, the current space for the battery pack does provide a space that allows for the battery to be removed easily, but it also limits the number of packs that can be placed in the scooter. If the scooter is to have more than one battery pack, both should be identical in order to make changing the battery easier. The current battery pack weighs around 5 kilograms and has an energy capacity of 10 amp hours at 36 volts, or 260 kilojoules per kilogram (compared to gasoline, at ~45 megajoules per kilogram). This is equivalent to roughly twenty to thirty minutes of drive time.

Forces Associated with a Bump

In order to determine the structure design that is able to support the specified loads attributed with the Roboscooter, the maximum forces on the scooter need to be calculated. The largest forces on the scooter will occur when the maximally loaded scooter is driving at maximum speed over a sharp bump with a height equal to the maximum specified bump size, which is determined by the amount of stopping force (force in the negative x direction) caused by that bump (see Figure 4).

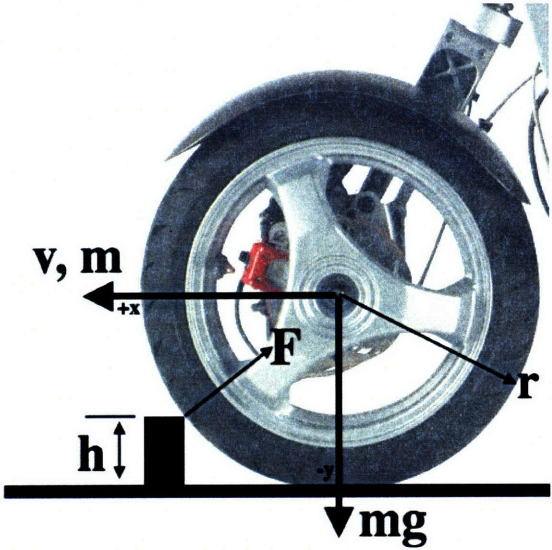


Figure 4: The free-body diagram of the front wheel of radius r as it goes over a bump of height h . Notice that the direction of the force the bump exerts on the tire causes a reduction in forward velocity as the wheel goes over the bump.

The heaviest components (battery and rider) of the scooter are horizontally positioned behind the main pivot and vertically just above the battery pack. Using this information the center of mass of the scooter can be determined, which will act as the pivot point of the structure when either wheel experiences the force of a bump. Also, the position of the center of mass determines the effective mass of the center of either wheel (using superposition) as it goes over a bump (see Figure 5).

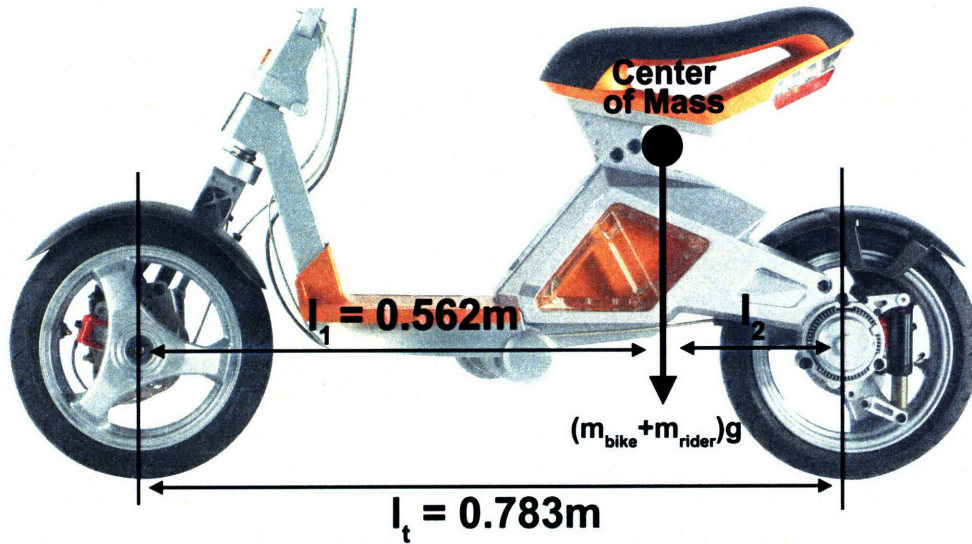


Figure 5: The location of the center of mass of the scooter determines the effective masses felt at either wheel. l_2 in this image is 0.221m.

As seen in Figure 4, a bump exerts both an upward, lifting force and a backward, stopping force on the wheel as it rides over the bump. Since these forces are much greater than the forces of a smooth road (only 1x gravity), they are used to determine the structural properties of the beams that make up the Roboscooter. In Figure 6 below, the forces (in g's) on the tire in the x and y directions are shown based on the dimensionless parameter h/r (bump height / wheel radius). As the bump height approaches the wheel radius, the force in the x direction – or the stopping force – increases dramatically ($F_x = -\infty @ h = r$).

In order to determine the force on the wheel, the angle of the force must first be determined. This can be done geometrically as seen in Equation 1,

$$\theta = \frac{\pi}{2} - \sin^{-1}\left(\frac{r-h}{r}\right), \quad (1)$$

which determines the angle between vertical and a line from the impact point with the bump to the center of the wheel, or a line perpendicular to the line tangent to the wheel at the impact

point. Using theta and the fact that the force moving the wheel over the bump must be greater than the downward force (mg) by $m \frac{d^2y}{dt^2}$, the upward force acting on the wheel is in terms of g is

$$F_y = 1 + r \cos\left(\frac{\pi}{2} - \theta\right) \frac{d\theta}{dt}. \quad (2)$$

since $\frac{d\theta}{dt}$ is simply $\frac{v_{scooter}}{r}$ when $v_{scooter}$ is held constant, Equation 2 becomes

$$F_y = 1 + v \cos\left(\frac{\pi}{2} - \theta\right). \quad (3)$$

Knowing the force in the y-direction and the angle of the total force on the wheel, the force in the x-direction can be calculated geometrically by

$$F_x = F_y \tan(\theta). \quad (4)$$

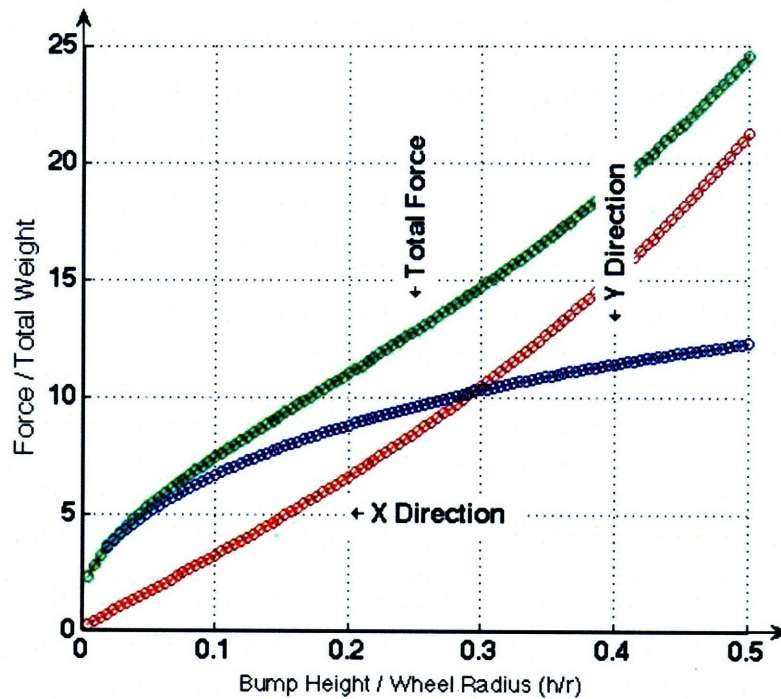


Figure 6: The forces (in g's) on a wheel of radius r in the x and y directions. Notice how the force in the x-direction approaches infinity as h/r increases.

Structural Analysis Based on Bump Forces

As can be seen in Table 1, the Roboscooter is designed to support 120 kilograms (265 lbs) under normal riding conditions, with a safety factor of two.

Table 1: Driving specifications for the Roboscooter based on the current design characteristics. The specifications that can change in future designs are the maximum speed (with a new drive system) and the maximum bump size (with different tires).

Specification	Value
Working Load	120 kg (265 lbs)
Maximum Speed	50 km/h (30 mph)
Safety Factor	2.0
Maximum Bump Size	3.6 cm (1.4 in)

The structural analysis of the scooter frame assumes rigid body constraints since the frame should ideally behave as a rigid body during travel. The maximum stress concentration is therefore easily determined using finite element analysis (FEA), which provides information on the current design's factor of safety taking into account the 5×10^8 cycle endurance limit of aluminum, which correlates to a maximum stress of 131MPa (See Figure 7).

By specifying a maximum stress that is at the industry standard "infinite" life of aluminum, chances of failure of the frame due to cyclic loading (due to bumps) are very low. Material defects or other uncontrollable conditions are the only factors that would allow a failure of this type to occur.

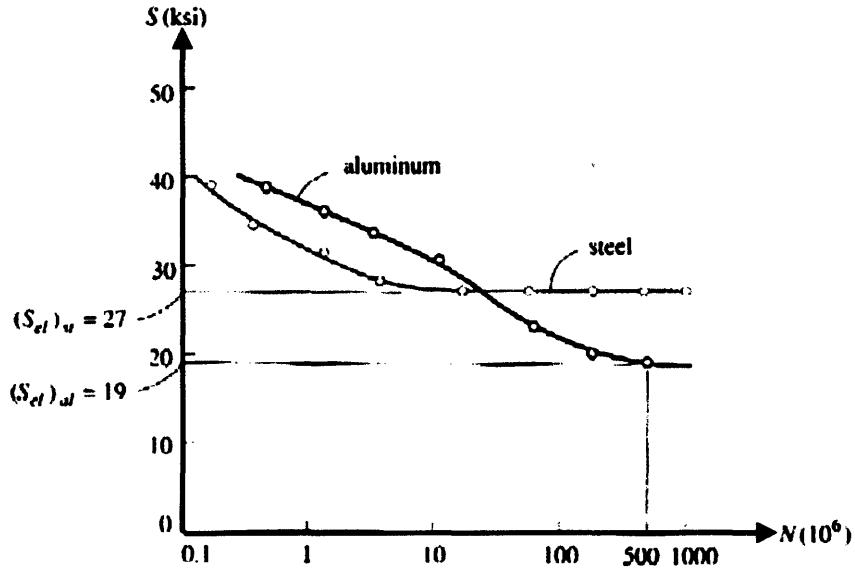


Figure 7: A typical S-N (stress vs. number of cycles) curve showing aluminum and steel.²

Most of the beams that make up the body of the Roboscooter are C-beams or channel beams. This type of beam offers strong shear and axial load resistance, but is somewhat weaker in torsion. Because it is important to reduce weight while having the necessary strength to support the scooter under loading, the relationship between the physical properties of channel beams and their strength under shear need to be well understood. In Figure 8 below, the factor of safety of a beam undergoing a constant load is compared to its weight. The outer dimensions, h and w , are held constant along each line. The increase in weight is due to an increase in wall thickness until the channel is the shape of a rectangular beam. Notice how, as the wall thickness approaches h or $t/2$ (whichever is smaller for given outer dimensions) the weight increases much more rapidly than the strength of the material.

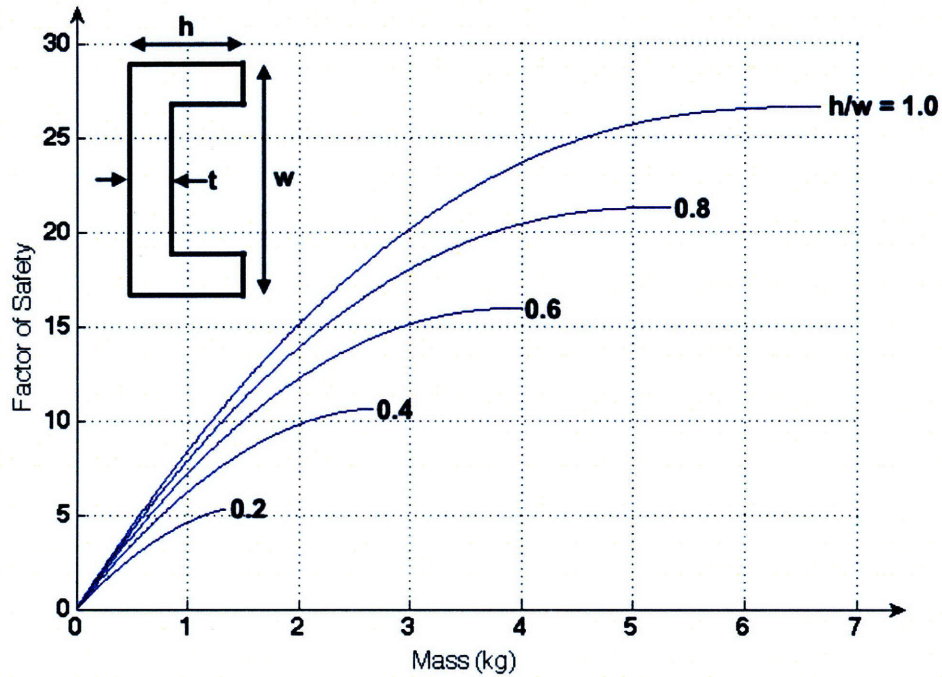


Figure 8: Factor of Safety versus Mass for a channel type beam undergoing loading due to a moment and its own weight. Each line increases with wall thickness, and ends when $t = w/2$ or h , whichever is smaller.

Alternatively, Figure 9 holds mass constant while varying w , h and t in order to show the geometric configurations that result in the most strength for a given mass. Since every point on each line represents a different configuration of the same mass, this figure is very helpful in determining the best channel beam to support a given load, although space and aesthetics may limit the choice of certain beams. It is also important to remember that this figure only shows the result of shear due to a moment about the x-axis. Certain configurations, even though strong in the direction shown, are very weak about y and/or z axis.

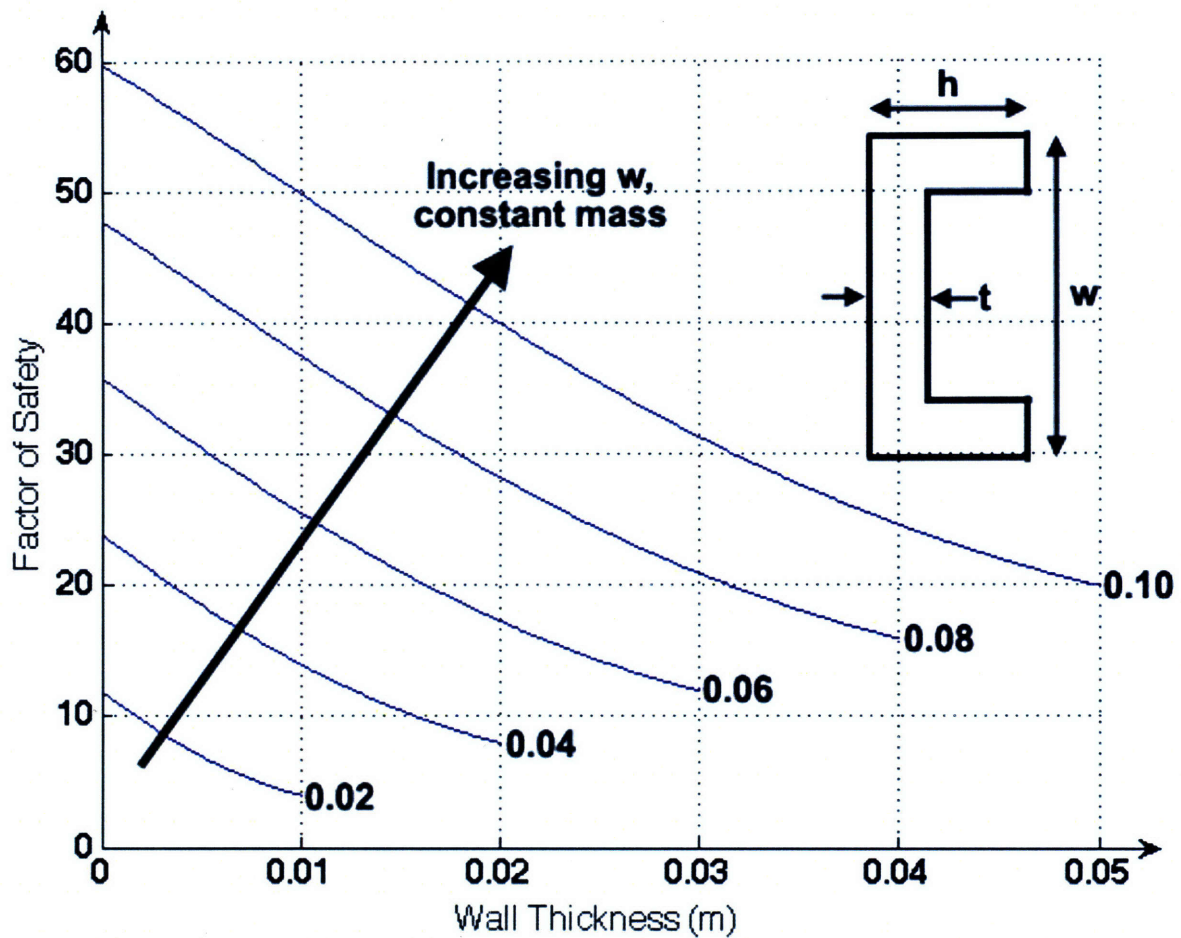


Figure 9: Factor of Safety versus Wall Thickness in terms of constant mass. The numbers labeling each line indicate w , which h being a function of both t and w .

The Front Fork

During a bump the scooter's front wheel experiences an 8.28g force in the y-direction and a 5.59g force in the x-direction (according to Figure 6). If the maximum specified rider mass is 120kg, then the total force at the center of mass of the scooter is 1765N, making the effective mass at the front wheel 498N. The combined loading conditions on the front fork can be seen in Figure 10. No moment exists at the wheel end (it is free to rotate).



Figure 10: Force diagram for the front fork. These are the maximum forces felt during riding conditions in which the scooter is traveling at maximum velocity over a bump of maximum height.

The front fork has a cross-section similar to that depicted in Figures 8 and 9. For this type of beam, the moment is equal to

$$I = \frac{t(w-t)^2}{2} \left(\frac{w-t}{6} + h \right), \quad (5)$$

and the area is equal to

$$A = t(w + 2h - 2t). \quad (6)$$

Using Equations 5 and 6 the normal force, shear force, and bending moment on the beam can be determined. For the normal force,

$$\sigma = \frac{P}{A} = \frac{4400N}{5.375 \times 10^{-4} m^2} = 8.196 MPa. \quad (7)$$

While the bending moment for the 573Nm moment, with c (the distance from the neutral axis) being as large as possible, or $w/2$, is

$$\sigma_{Moment} = \frac{Mc}{I} = \frac{573Nm \cdot 0.063}{2 \cdot 3.065 \times 10^{-7}} = 58.89 MPa. \quad (8)$$

For the shear stress in the front fork, the 2310N of shear force cause a stress of

$$\tau_{max} = \frac{VQ_{max}}{It} = \frac{2310N \cdot 5.676 \times 10^{-6} m^3}{3.065 \times 10^{-7} m^4 \cdot 5.0 \times 10^3 m} = 8.555 MPa. \quad (9)$$

Using stress transformation equations to find the principle stresses on the front fork, the conditions for yielding based on the maximum-distortion-energy theory are

$$\sigma_{1,2} = \frac{\sigma_x + \sigma_y}{2} \pm \sqrt{\left(\frac{\sigma_x + \sigma_y}{2}\right)^2 + \tau_{\max}^2}$$

$$\sigma_1 = 68.16 \text{ MPa}$$

$$\sigma_2 = -1.07 \text{ MPa}$$
(10)

The maximum-distortion-energy theory states that $(\sigma_1^2 - \sigma_2^2)$ must be less than the yield strength squared of the material, or in this case the infinite cyclic fatigue limit, which is 131MPa squared. Solving shows that while $(\sigma_1^2 - \sigma_2^2)$ is 4.72GPa, the yield limit of the aluminum front fork is 17.2GPa, giving the current design a safety factor of 1.91 (after taking the square root), which is within tolerable error of 2.0. For a check, the safety factor using maximum-shear-stress theory was also calculated to be 1.89.

Because the front fork handles a very large load, the current design appears to fit with analysis as appropriate. There are, however, several changes to the beam design that would improve its structural stability without increasing weight. Currently the channel opening faces toward the wheel. There is a small moment about the y-axis created by the offset wheel (neglected in the above calculations because it is small). Upon yield due to normal or bending moments, this y-axis moment could contribute to more rapid failure due to the channel wall flanges being under compression rather than tension, which would allow them to simply bend due to shear flow. The current front fork design does implement internal webbing to prevent this from happening, but a more elegant design would reverse the direction (rotate 180 degrees about the z-axis) of the channel and use a non-structural cover for front aesthetics.

The Main Pivot

The force on the main joint is very high, and it is therefore important that the bearings and axles that make up the joint are properly sized. Taking the scooter frame as a simply

supported beam with a concentrated rider and battery force at the center of mass, we can see that the x-axis (horizontal) distance from the rear wheel center to the point of force (b) is smaller than half the wheel-base, or over the center of mass of the vehicle. The moment acting on the main pivot due to this force is

$$M = \frac{-PbL}{2}. \quad (11)$$

From Equation 5 and the fact that the main pivot lies 0.041m below the neutral axis of the scooter's frame, we can see that the force on the main pivot shaft is

$$F = \frac{M}{c} = \frac{1765N \cdot 0.61m \cdot 1.42m}{2m \cdot 0.041m} = 18600N. \quad (12)$$

From this we can calculate the maximum moment on the steel shaft connecting the two halves of the scooter geometrically by

$$M_{shaft_{max}} = \frac{F_{shaft}}{2l_{sep}} = \frac{18.6kN \cdot 0.054m}{2} = 502Nm. \quad (13)$$

Since this design is based upon maximum-shear-stress theory knowing the allowed shear stress $\tau_{allow}=186MPa$, we can determine the necessary diameter of the shaft directly by

$$\begin{aligned} d &= 2 \left(\frac{2}{\pi \tau_{allow}} \sqrt{M^2 + T^2} \right)^{\frac{1}{3}} = 2 \left(\frac{2}{\pi 186MPa} \sqrt{502Nm^2} \right)^{\frac{1}{3}} \\ &= 0.024m = 2.4cm \end{aligned} \quad (14)$$

The current shaft in the main pivot is consistent with this calculation, having a diameter of 2.4cm. The main pivot shaft size can be reduced further by decreasing the separation between the bearings in the main pivot, though, because of the cubic relationship, a 50% reduction in separation distance will equate to only a 20% reduction in shaft diameter. Decreasing the separation distance has other benefits as well. A wider contact region with the main pivot shaft

will provide more stability against moments acting about the y-axis (vertically upward) of the scooter.

Additional Design Comments

The front fork and main pivot are focused on in this analysis because they experience the largest forces during riding. The other beams that make up the scooter, however, have a much higher inertial moment and therefore have a much higher factor of safety. In particular, the pair of beams connecting the front fork to the main pivot has just over double the inertial moment (in its weakest places) of that of the front fork. For this reason, these beams can be reduced in size such that they experience more fully stressed conditions under maximum loading, taking into account the safety factor, cyclic loading, and moment multiplication properties associated.

Most importantly, the set of twelve beams that comprise the battery pack area is vastly over-engineered. Due to manufacturing limitations for the proposed aesthetic design these beams are much heavier than they need to be in order to support the loads required even under maximum stress. Also, reduction of material in this area will allow for an increase in both battery and storage capacity.

Currently the Roboscooter makes use of an all aluminum alloy frame. At the cost of a higher price, substitution or composite beams of other, lighter and equal strength materials can be used in the design of the scooter frame. Most notably, certain magnesium alloys have a similar strength in comparison to aluminum, with roughly 30% less weight. Also notable are composite materials such as carbon fiber, but these materials have a strong aesthetic drawback, and are much more costly even in comparison to magnesium alloys.

While the Roboscooter is currently very structurally sound, it is in some places too much so. In order to reduce the weight of the scooter further it is necessary to accurately gauge the forces on each beam that makes up the structure so that the most structurally optimal solution can be obtained. Through new material and structural investigations, the Roboscooter will be able to have both the portability and driving range necessary to enter the new exclusively electric one way user-share market successfully.

References:

- [1] Hildebrand and Wolfmüller, "Motorcycle," German Patent 78553, Jan. 20, 1894.
- [2] R.C. Hibbler. *Mechanics of Materials*. New Jersey: Pearson Prentice Hall, 2005.
- [3] Material Specifications. *MatWeb* Automation Creations, Inc. Blacksburg, VA, 2008, <http://www.matweb.com>.
- [4] The Aluminum Association, Inc. *Aluminum Standards and Data 2000. International Alloy Designations and Chemical Composition Limits for Wrought Aluminum and Wrought Aluminum Alloys*, 2001.
- [5] Lin, Michael. (private communication), 2008.